An Ad-Hoc Capture System for Augmenting Non-Digital Water Meters

Nils Schwabe
Albert-Ludwigs-University
Freiburg, Germany
schwaben@tf.uni-freiburg.de

Philipp M. Scholl
Albert-Ludwigs-University
Freiburg, Germany
pscholl@ese.uni-freiburg.de

Kristof Van Laerhoven
Albert-Ludwigs-University
Freiburg, Germany
kristof@ese.uni-freiburg.de

ABSTRACT

Deriving more detailed insights into one's ecological footprint is a premise to reduce one's individual environmental impact. Personal water consumption contributes significantly to this impact, but remains hard to quantify individually unless digital meters are installed. In this paper, we present a dual-sensing approach to retro-fit common water meters with a wireless sensor unit that is able to capture an individual's water usage, and digitally forward it over the home's WiFi network. Utilizing active infrared distance sensing or sensing magnetic flux, it is possible to measure water consumption with an accuracy below $0.1l$ on commonly installed meters. With a continuous power consumption (assuming a daily water consumption of 2 hours) of less than 20 mW, the system can be provide real-time feedback to home-owners, office workers and people sharing such a retro-fitted water supply.

ACM Classification Keywords

H.5.m. Information Interfaces and Presentation (e.g. HCI): Miscellaneous

Author Keywords

digital water meter; eco-feedback; sensors;

INTRODUCTION

Analog water meters are the sensing part of a ubiquitously employed technology to track water consumption across large water services. Deployed at each larger water supply tap, they are used by utilities to measure the overall water consumption of smaller entities, such as individual households or companies. The quantity of used water is regularly read out on the water meter by the water company. Often, these water meters are placed at positions that are not easy to access—for instance in the basement or under a staircase. The water consumption is as a result not very transparent to the consumer, who is only informed about his or her usage over the last period. Figuring out which activity is related to which amount of consumed water, and related to this which amount of energy was required to provide hot water and neccesary water pressure, is complicated by this fact. A digital water meter that is connected to a local network and a central application responsible for capturing and presenting the data can help the consumer to get a better understanding of his or her water consumption [1]. Moreover, time and money can be saved by automating the meter-reading.

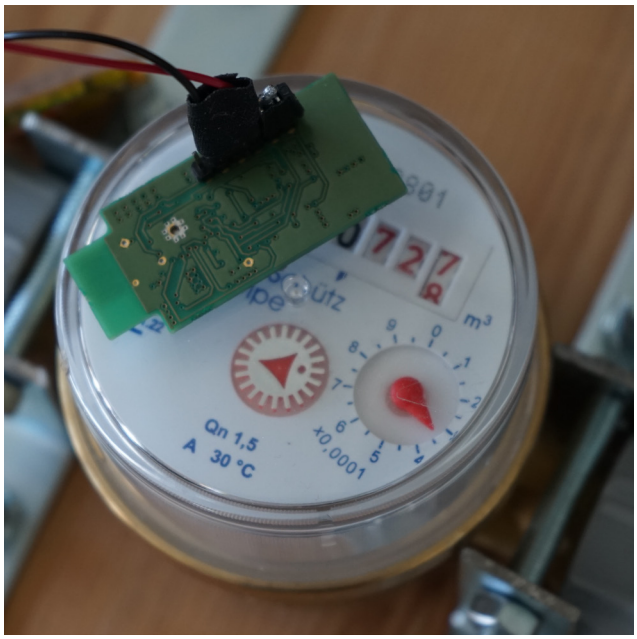

Figure 1. WiFi-connected device placed on a common water meter, which estimates water usage from the readings of a built-in magnetometer and active infrared sensor. It is compact and energy-efficient enough to be installed quickly for prolonged periods of time, and is able to provide continuous water usage readings.

The applications of a locally-networked and digital water usage meter are manifold. Apart from the ability to log water consumption in more detail, the digitally acquired data can also be displayed in real-time on displays or devices that are placed near water-consuming appliances, such as water taps, washing machines, or garden equipment, across networks following the *Internet of Things* paradigm. In doing so the user is directly confronted with

IoT'16, November 07 - 09, 2016, Stuttgart, Germany

ISBN 978-1-4503-4814-0/16/11…$15.00

DOI: http://dx.doi.org/10.1145/2991561.2991576

his water consumption, provided with eco-feedback [2]. The design presented here can be easily integrated into existing WiFi networks, and can also serve as the foundation of do-it-yourself solutions.

The contributions of this paper are threefold: First, we introduce two sensing modalities to continuously capture and estimate the water usage readings from a common water meter. Second, we compare different signal processing methodologies, and show the attainable accuracy for estimating continuous water usage with the two sensors. Third, a straightforward and easy to configure method is demonstrated to install this device effortlessly in a new environment on top of a legacy water meter, through a local WiFi network.

In the next section, we situate our work within the state-of-the-art techniques and propsals to measure water consumption, and enumerate the main differences to our approach.

RELATED WORK

Digital Water Metering Methods. Several methods have been proposed to digitally measure water usage in the past decades. The first type, electromagnetic flow monitoring, is based on Faraday's law of induction, in which an electro-magnetic field is applied to a non-magnetic part of the water pipe. This requires the fluid to be conductive, i.e. the water needs to contain ions. The magnetic field then deflects the charge carriers to either side. This creates a difference of potential orthogonal to the direction of the magnetic field. The flow can then be measured using two electrodes placed on each side of the pipe [3]. An advantage of this system is that no mechanical parts are neccesary, however a part of the pipe needs to be swapped and such a meter system generally cannot be fitted onto an existing water pipe.

Ultrasonic flow meters are a second option, with the most common type based on the Doppler Effect in that sound waves move slower against a fluid stream. Two ultrasound transceivers are plugged onto an existing water pipe and one wave is sent in the direction of the flow and one in the other. The runtime difference of the two signals is related to the flow rate [4]. This method has an advantage over the electromagnetic flow meter since it can be placed directly on top of any existing pipe. It is however very sensitive to calibration inaccuracies and is required to be firmly attached.

Alternatively, optical character recognition (OCR) with a video camera can be used [5]. This approach is rather complex, demands constant lighting conditions which requires greater installation effort, and consumes a lot of energy. However it provides measurements on par with the ones the analog display of the water meter provides.

The fourth alternative generates a flow rate signal via mechnical means. A propeller installed in the water stream, relates its rotation to the actual flow rate. Such a setup can also be used to harvest energy to drive the actual sensor [6]. However it needs to be installed into the water supply system, which when not installed directly at an easily-removed tap, present quite an effort.

Smart Meters. As defined by the European Standard *EN14154*, smart meters should include: "improved communication with the consumer, alarm facilities for leakage or tampering/manipulation, as well as the ability for multiple readings at set time intervals" [7]. A water meter that is considered "smart" typically includes interaction abilities with its environment. Wireless communication and storage capabilities are therefore often provided, especially since data is recorded in greater detail, compared to a conventional water meter. Activities can be related to water usage, either via timestamped readings or by means of a live display [6, 7]. This is not possible with the current procedures followed by water utility companies, where customers usually receive a bill containing the overall usage after multiple months.

Smart metering is considered to play a central role in reducing water usage in domestic environments [2, 7]. Multiple studies have pointed out that smart metering and its related possibility for the user to access his or her usage via a computer, smart phone and in-home display can have a positive impact on water usage [8]. Providing direct feedback to the consumer might explain this [6]. Smart meters also extend the metering in a way that the water usage readings are not delayed, but can be accessed in real-time or near real-time. This helps the user to instantly obtain feedback and offers further opportunities to react. A further feature of smart metering is the ability of the water supplier to let the consumer pay in shorter intervals and for exactly that amount which was consumed [7].

As described by Sønderlund et al. [1] there are different ways to inform the user about water usage. These are for example: web-based, in-home displays and mail-based. These methods proved to be very different in effectiveness. Most effective seemed to be information that is delivered at the point in time when it is used including advices to reduce consumption. However, all of these methods require a smart meter that can be used as a source of data.

Commercial Products and Solutions. With the advance of wirelessly-connected sensors for the home environment, several commercial products have been emerging to digitally monitor water usage. The *Driblet* [9], for instance, is a device which is installed in between two water pipe segments. It is self-powered, transmits data in real time via WiFi, the data is accessible via a web interface and a mobile app. One big advantage of this device is that it harvests its energy from the water flow. However, this also requires a less than straightforward installation, often in locations that might not be easily accessible. The *FLUID* [10] uses a mobile app to communicate with the user. It is also called "The Learning Water Meter" as it is able to automatically differentiate appliance's water usage. Using the app, usage patterns can be taught that the device which is then able to recognize these

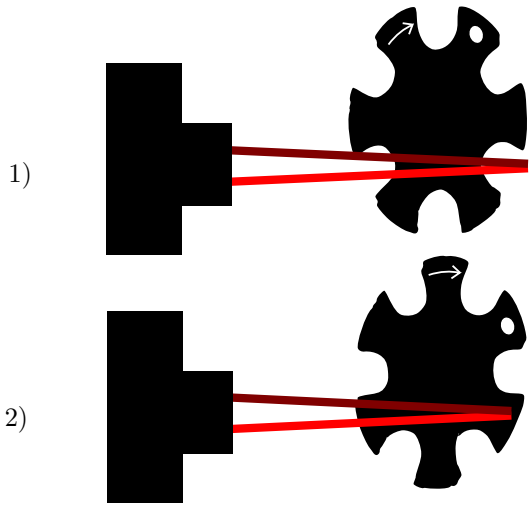

Figure 2. Using an active Infra-Red (IR) sensor to measure the position of the cogs of the fine-grained measurement dial on top of a water meter. Such dials can be found in the majority of commonly deployed water meters.

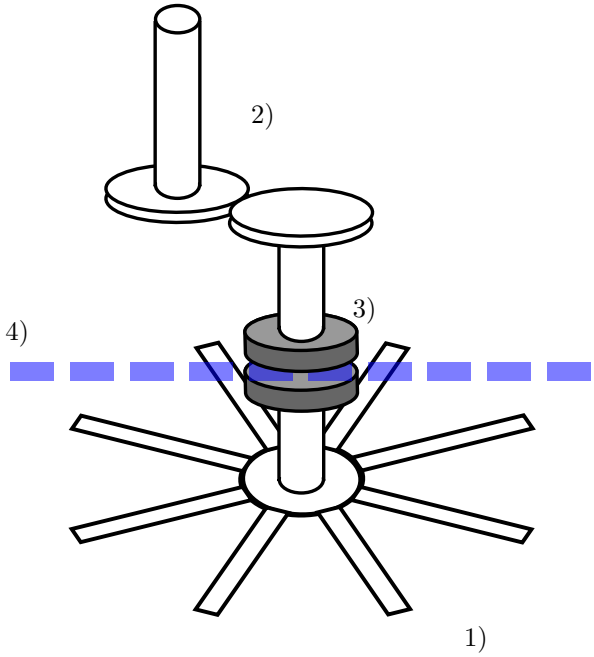

Figure 3. Magnetic coupling in water meters is used to separate the inner parts between a dry and a wet area. The magnets that are used produce a periodic magnetic field that is measureable. 1) Impeller; 2) Gears; 3) Magnetic coupling; 4) Separation of wet and dry area. This type of coupling is found in most non-plastic legacy water meters.

scenarios, as well as leakage detection. The device itself uses the method of ultrasonic flow meters and can be plugged on an existing pipe which is a huge advantage. A disadvantage is that the device is powered by a mains power supply which means that it cannot be placed at any location. Another system, still under development, is made to replace traditional water meters. The *IntelliH2O* [11] is able to measure water usage, temperature and pressure. The device is powered by a rechargeable battery. Furthermore, the device is capable of controlling an integrated valve (on/off). This way, the valve can be opened to prevent the water pipes from freezing, and a display allows its users to read water consumption data.

Our system differs significantly to these prior works in application, as it does not require the original water infrastructure to be altered: pipes do not need to be removed and existing (and calibrated) water meters can remain in place. We argue that, as a result, installation of our system is straightforward and, given that it is energy-efficient enough to operate over longer stretches of time, effortless to maintain. As our system estimates water consumption by continuously monitoring the common water meter's dial, however, we do need to ensure that the estimates of consumed water are indeed accurate enough. The remainder of this paper will first present our approach and illustrate it by a compact and fully functioning prototype, after which we evaluate and discuss its performance.

SYSTEM DESIGN AND IMPLEMENTATION

The developed device uses an *ESP8266* micro-controller by *Espressif Systems*, the inertial measurement unit *BMX055* by *Bosch*, which includes a compass unit, and the infra-red distance sensor *VCNL4010* by *Vishay*. The main reasons why this micro-controller was chosen are that it features integrated 802.11 b/g/n WiFi connection using a PCB trace antenna and its stand-by power consumption of less than 1 mW. An mDNS [12] responder was set-up to provide infrastructure-less name resolution and service discovery. The data is received by a Javascript web app using Websockets [13].

To acquire the current water consumption of an analog water meter, two methods are considered. In the first one an infra-red based distance sensor tracks the rotation of a gear on top of the water meter (see Figure 2). The second method tracks water consumption by measuring a side effect of the magnetic coupling which is used in many water meters. Figure 3 illustrates the function of a magnetic coupling which separates the internals of a water meter into a dry and a wet area. The magnetic field of the coupling can be measured outside of the water meter which is done using a magnetometer.

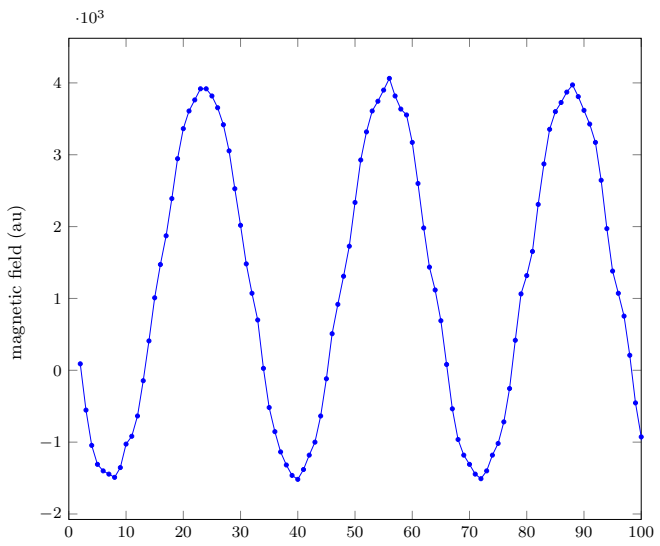

Figure 4. Unfiltered measurement of the magnetic field using a sampling rate of 75 Hz. The magnetometer was placed directly on top of the water meter.

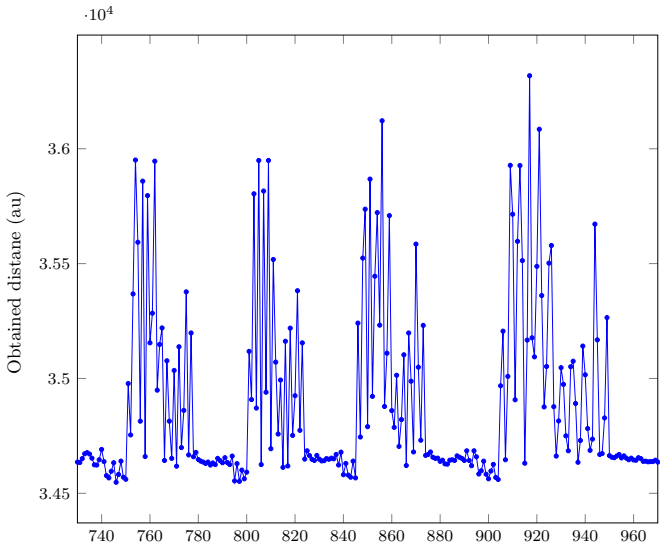

Figure 5. Unfiltered measurement of the infra-red sensor at a sampling frequency of approximately 80 Hz. The sensor was placed above the small wheel as shown in Figure 2.

Both sensor exhibit measurement noise from the digitalization steps. To remove this a smoothing algorithm is applied: a window of N samples is extracted and the $15th$-percentile is removed. Different values of N were examined and a value of $N = 7$ produces a sufficient result which contains almost no noise. To remove the constant offset of the signal, the derivative is calculated using the central difference in Equation (1). h is chosen to equal one sample. This can be done since the important part of the signal is the frequency which does not change when taking the derivative:

$$\frac{df}{dx}(x_0) = \frac{f(x_0 + h) - f(x_0 - h)}{2h} \tag{1}$$

$$\begin{aligned} f(x) &= a \cdot \sin(b \cdot x + c) + d \\ \frac{df}{dx}(x) &= a \cdot b \cdot \cos(b \cdot x + c) \end{aligned} \tag{2}$$

A signal with a peridiocity of $b \cdot x + c$, amplitude a and a constant offset d, can be described according to Equation (2). Deriving Equation (2) removes the constant offset, changes its amplitude but does not change the frequency of the signal, which stays at $p = \frac{2\pi}{b}$. The frequency of the signal, or rather the rate of turn of the observed wheel, is the signal attribute that actually gives a measure of the water flow. To extract the water flow we have to look at the signal of each sensor separately now.

Magnetic Data

The graph of the measured signal (depicted in Figure 4) is similar to a sine wave. The periods which last roughly 40 samples in this example correspond to one spin of the magnet inside the magnetic coupling. To measure the water flow, and with that consumed water volume it is sufficient to count these periods. Typical flow speed in a house-hold were tested and the frequency varies between 2 Hz and 20 Hz. Three methods were compared to extract the current frequency; Fast Fourier Transform, Goertzel's algorithm, and zero-crossings.

The Fast Fourier Transformation offers the most accurate spectrum, however also require heavy processing. A faster alternative is Goertzel's algorithm, which can be efficiently computed, however only a limited number of frequencies can be checked for. Zero-Crossings only estimate a single frequency per period [14]. This requires the removal of the constant signal offset and of noise. Furthermore, due a limited sampling frequency, the exact location of the zero level needs to be estimated as well. The *intercept theorem* as depicted in Figure 6 allows for that. These methods are discussed in Section 4

Infra-red Data

The signal acquired with an infra-red distance sensor is shown in Figure 5. The peaks occurring approximately every 50 samples correspond to the pass of one spike. An analytic method was developed to determine the signal frequency. The goal is to find local maxima, or peaks, in the recorded data. For this the first and the second derivative are calculated. Zero-crossings in the first derivative are determined, and minima filtered out using the respective second derivative at this point. The differentiation is realized using the central difference in Equation (1). A smoothing step is required to harden this method against noise and short peaks. Afterwards the rate of turn can be determined as the time between two such identified peaks.

EVALUATION

To compare the different measurement techniques, a test set-up was built. This system consists of a controllable

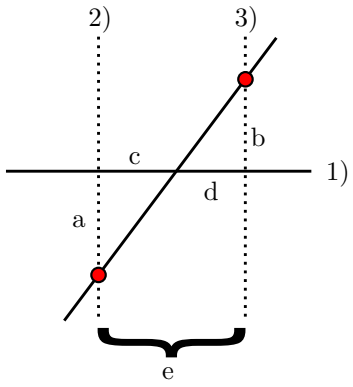

Figure 6. Illustration of two samples (red dots) around a zero-crossing. The intercept theorem is used to approximate it. 1) x-axis; 2) sample$_{i-1}$; 3) sample$_i$; a and b values of the samples; c and d need to be calculated; e distance between two samples.

water pump, a small water tank and a typical water meter. Thus water flow can be simulated by pumping water through the water meter at different speeds.

Comparing the Signal Processing Techniques

To compare the results in a reasonable way, the test data was recorded using the magnetometer and the infra-red sensor simultaneously. Figure 7 shows the magnetometer data, Figure 10 shows the infra-red data. The following discussion, which compares different processing techniques, refers to this common test data.

Fast Fourier Transformation (FFT)

The algorithm was used on raw test data shown in Figure 7. The graph of the measured signal shows that the water flow was started at sample number 200 and stops slowly after approximately 950 samples. The analysis using the Fast Fourier Transformation (cf. Figure 7 bottom) reveals two major frequencies. The first bin is located at a frequency of 0 Hz which is due to the static offset. The second bin is located at 2.143 Hz which corresponds to the frequency generated by the rotation of the magnetic coupling.

The main advantage of this algorithm is accuracy. The resolution is limited by the sampling frequency and the amount of samples: $\mathrm{df} = \frac{f_s}{n}$ [15]. Using the test data, it turned out that a minimum of 500 samples was needed to gain sufficient accuracy of $b = \frac{f_s}{N} = \frac{75\,\mathrm{Hz}}{500} = 0.15\,\mathrm{Hz}$. That means that a comparatively large interval must be kept in memory, i.e. about 2 kB. Furthermore, its computational complexity lies in $\mathcal{O}(n \log n)$ where n is the number of samples [15]. While the *ESP8266* provides enough RAM, the simultaneous handling of data processing and WiFi connection is challenging.

Goertzel Algorithm

This algorithm calculates the spectral amplitude of a single frequency. For that it only requires n multiplications and $2n$ additions for each spectral component, with n being the number of samples [16]. Similar to the

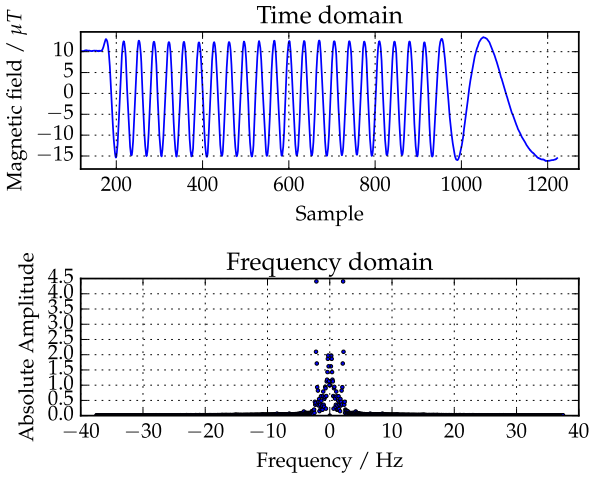

Figure 7. Fast Fourier Transformation (bottom) on a sample magnetic field signal (top). The highest bin is located at a frequency of $f_{res} \approx 2.143\,\mathrm{Hz}$.

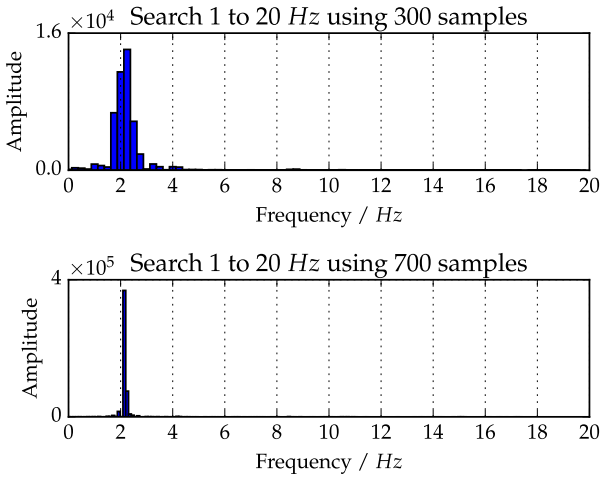

Figure 8. Two cycles on the test data set using the *Goertzel Algorithm* and different amounts of samples. The bin width of the first graph is $b = \frac{f_s}{N} = \frac{75\,\mathrm{Hz}}{300} = 0.25\,\mathrm{Hz}$ which means that 80 frequencies were scanned. The highest bin is located at $f_{res} = 2.25\,\mathrm{Hz}$. The bin width of the second graph is $b \approx 0.107\,\mathrm{Hz}$ which means that 187 frequencies were scanned. Its highest bin is located at $f_{res} \approx 2.143\,\mathrm{Hz}$.

FFT, its accuracy is limited to the amount of samples n and the sampling frequency f_s: The bin width of this algorithm can be calculated as $b = \frac{f_s}{n} = \frac{75\,\mathrm{Hz}}{700} \approx 0.107\,\mathrm{Hz}$. This means that accuracy of the results is 0.107 Hz which can be seen in the second cycle in Figure 8. To further increase the accuracy, more samples are required, which again increases the amount of required storage space.

Using the *Goertzel Algorithm*, rather than the *FFT*, only makes sense if the number of spectral components to check for is known upfront and can be limited. In comparison the *Goertzel Algorithm* is only faster if less than $\log_2 n$

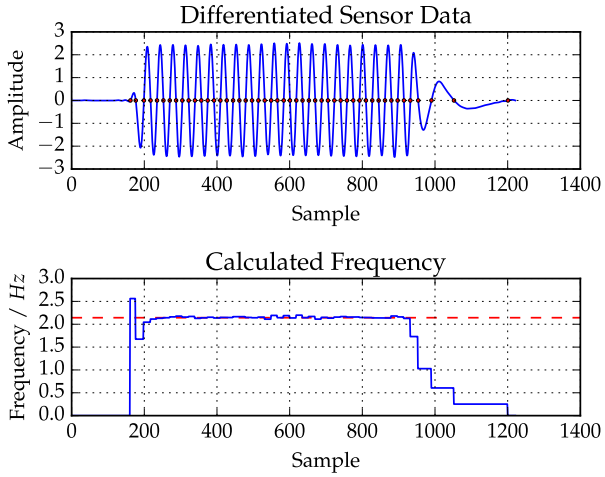

Figure 9. Results of the method using zero-crossings. The change of the amplitude is due to the differentiation. The red dots depict the recognized zero-crossings (top) which are then used to calculate the period T and the frequency (bottom). The red dashed line depicts the frequency of 2.143 Hz calculated using the *Fast Fourier Transformation*.

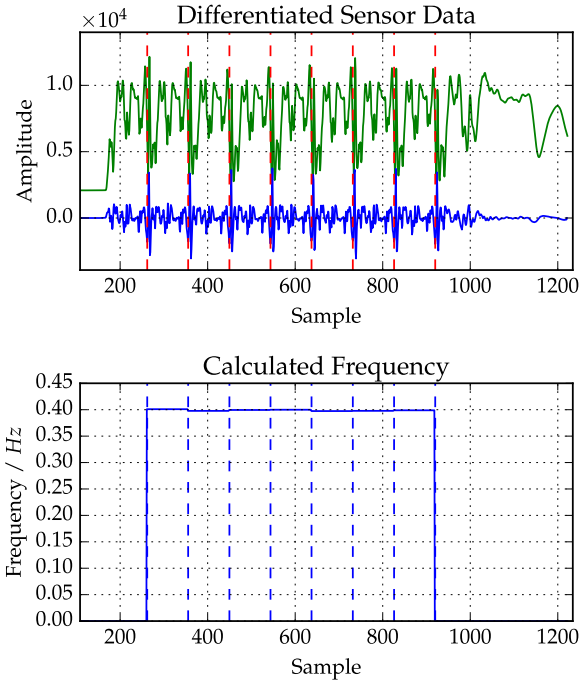

Figure 10. Results of the zero-crossing algorithm applied on the test set for infra-red data. The signal (green) was differentiated (blue) and analyzed for turns of the wheel (red). It can be seen that not all turns are recognized correctly. Specifically peaks at the beginning and end of the recordings are not recognized, probably due to current phase of the cogs on the wheel.

spectral components are calculated [17]. In the case of 700 samples this would result in $\log_2 700 \approx 10$ spectral components. Only ten different water flow speeds could be detected, which would be a rather rough estimate. Especially given the fact, that this speed needs to be integrated to get the actual water consumption.

Zero-Crossings

The last technique works surprisingly well. It is very suitable since it is able to compute the frequency of the signal within every half of a period. The computation can be done on the fly meaning that only four consecutive samples s_i to s_{i+3} and the time-stamps need to be saved. To calculate the differentiation of s_{i+1}, the samples s_i and s_{i+2} are used (cf. Figure 6). Which can be achieved with three comparisons, five additions and two multiplications. This approach is however less accurate than the *FFT*. The results of this approach can be seen in Figure 9. The first graph shows the differentiated signal and the second shows the computed frequencies between the zero-crossings which are the minima and maxima of the signal.

A further advantage is that the method can be applied to the infra-red data with minimal preprocessing. The results in Figure 10 show that the algorithm does not recognize all spikes correctly which implies mistakes in the calculation of the frequencies.

Table 1. Comparison of the methods: n amount of samples, m amount of spectral components, T signal period, f_s sampling frequency

	Fast Fourier Transformation	Goertzel Algorithm	Zero-Crossings
Accuracy	$b = f_s/n$	$b = f_s/n$	
#Samples	500 to 700	500 to 700	n in $T/2$
Complexity	$\mathcal{O}(n \log n)$	$\mathcal{O}(m \cdot n)$	$\mathcal{O}(n)$

Calculating Water Consumption

Since the *zero-crossing* method requires the least amount of computation, can be calculated by the MCU during measurements, and can be easily applied to both signals, it is used for further analysis. The method used to calculate the water consumption out of the recognized zero-crossings is the following: every zero-crossing represents one turn of the wheel and thus can be multiplied by an appropriate factor $a_{mag/ir}$. This factor is determined by calibrating the system. It indicates the water volume passing the wheel after one rotation. To achieve this, a known water volume w_{vol} is passed through the system while the number of rotation n_r is counted. The calibration factor can be then determined as $a_{mag/ir} = \frac{w_{vol}}{n_r}$. The counted turns are then summed up which leads to a consumption graph as shown in Figure 11. In the figure, the two sensor modalities are compared concerning the total water consumption.

Accuracy

Several test cycles were done in order to verify the accuracy of the system. Therefore a test system with a controllable pump was used and a defined volume was let pass during the measurements. In Figure 12 the results of a test run are shown where a 500 mL beaker glass was

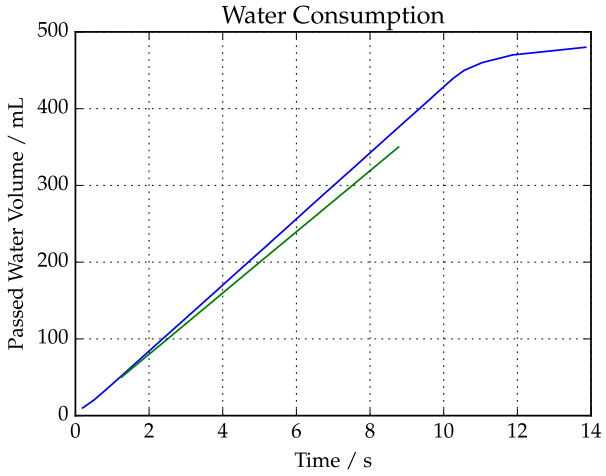

Figure 11. The same test data as before was used to calculate the water consumption of the magnetic (blue) and the infra-red (green) data. The factors were calibrated to $a_{mag} = 10\,\mathrm{mL}$ and $a_{ir} = 50\,\mathrm{mL}$. A total amount of $500\,\mathrm{mL}$ was passed. It is noticeable that the consumption calculated using the infra-red sensor is incorrect. The reason for that is that two spikes (equal to $2{\cdot}50\,\mathrm{mL} = 100\,\mathrm{mL}$) were not recognized which can be seen in Figure 10. These are the rotation when opening and closing the valve.

filled with a fixed speed for eight times. The maximum variance of the final consumption is 10 mL or 2 %. This can have two different reasons. At first it could be possible that one zero-crossing was not recognized which leads to a variance of a_mag which was calibrated to 10 mL in this case. Secondly, the beakers were filled manually which can lead to different volumes in the test runs.

Several test runs were performed using different volumes and speed. The results strengthen the assumption that the system has a accuracy of 2 % using the magnetic method. The infra-red method (cf. Figure 13) in contrast shows a maximum variance of the final consumption of 100 mL or 20 %. This is due to factor a_{ir} calibrated to 50 which would mean that two rotations were missed.

Comparing Magnetic And Infra-Red Measurements

Data acquired using a magnetometer is more accurate than acquired with an infra-red sensor. This can be said since the two measurements were done simultaneously. A very important advantage of the infra-red based method is that almost every water meter features a usable wheel on its front. A magnetic coupling in contrast is not used by every water meter. However, the infra-red processing technique is currently too simple and needs to extended to handle the cases during opening and closing the tap.

Energy Consumption

To asses the energy consumption of the system we introduce two states: *standby* and *communicating*. In *standby* only the sensors are powered. Both support to assert an interrupt line, once the sensor value is below or above a threshold. This line can be used to wake the processor of

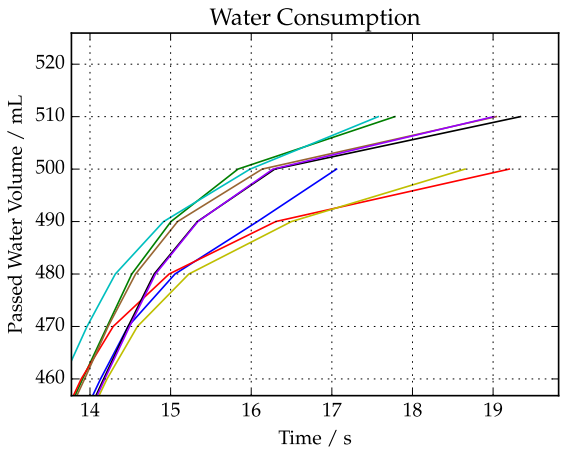

Figure 12. This is a closer view of a graph similar to the one in Figure 11 to compare the accuracy of eight magnetic measurements. The data was acquired while filling a $500\,\mathrm{mL}$ beaker glass with a fixed speed. It can be seen that the maximum variance is $10\,\mathrm{mL}$. This variance can be due to the fact that the beakers were filled manually.

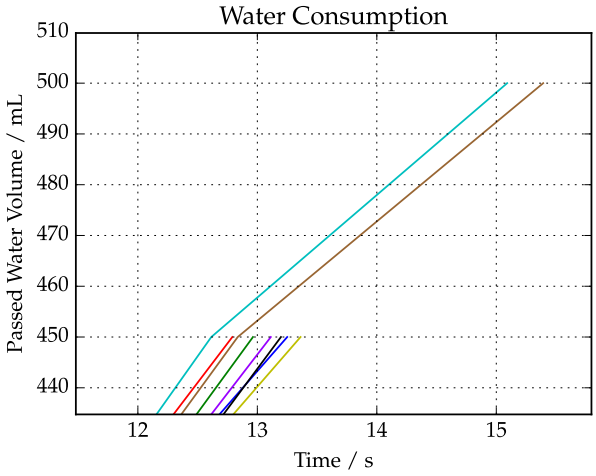

Figure 13. This graphs shows eight measurements of the infra-red signal. It is visible that in six cases, the last peak of a rotation were missed. Therefore $50\,\mathrm{mL}$ are missing from this consumption

the ESP8266 platform which has a stand-by consumption of 1 mW. Depending on the usage profile this state is most often attained. Added to this are the standby consumption of 1.65 mW for the magnetometer, and 6.6 mW for the infra-red sensor. Which in total requires 2.65 mW or 7.7 mW during *standy*.

The *communicating* state is attained once the microprocessor has been woken up. In this state, sensor data is transferred to the micro-processor and further processed. Simultaneously, the WiFI connection is started to advertise the monitoring service and to eventually transmit data to other stations. This requires 280 mW.

With the chosen real-time model, *sensing* and *communicating* are always done simultaneously, requiring a large amount of energy. If we assume a daily measurement/consumption time of 1.5 hours, the energy daily energy consumption can be estimated. For the magnetometer, this would total to a consumption of $1.5\,\mathrm{h} * 280\,\mathrm{mW} + 22.5\,\mathrm{h} * 2.65\,\mathrm{mW} = 479.6\,\mathrm{mW\,h\,d^{-1}}$ or $\sim$20 mW on average. For the infra-red sensor, the average amounts to $\sim$24.7 mW.

Assuming a li-ion battery capacity of 400 mA $\approx$ 1500 mW, a run-time of 2 to 3 days is possible. Switching to a different wireless transmission technology, while provinding less convenience, could increase the runtime significantly. The WiFi transmission requires 85 mA, while a typical IEEE802.15.4 or Bluetooth connection requires around 20 mA. This would result in an average power consumption of $\sim$6.6 mW for the magnetometer, and $\sim$11.3 mW for the infra-red sensor, or a runtime 5 to 10 days. A further opportunity for reducing the power consumption would be to decrease the standby consumption by adapting the sampling rate.

Limitations of the System

A general limitation which is implied by the sampling frequency is the maximum flow rate determined by calculating $Q = a_{mag/ir} * f_s \geq 500\,\mathrm{mL\,s^{-1}}$. It can be improved by picking sensors that are able to sample at a higher rate. Secondly, the magnetic measurements is sensitive to external disturbances, like permanent magnets or electronic devices. A final limitation is the calibration process, since it determines the accuracy of the whole system. If it is not correctly done, all further results will contain a systematic error. This can later be corrected with a repeated calibration. For example by comparing the analog water consumption display by the value given by the digital meter.

While the magnetic sensor can be placed anywhere in the varying magnetic field, which is nearly at each spot on the water meter, the infra-red sensor is not so simple to install. For it to work at all it needs to have a clean sight of the cog of the wheels. This is harder to install, however one could imagine a system where the user moves the sensor around until it picks up a signal while the water is flowing through the tap.

Finally, the major limitation of the current system is power consumption. This could be mitigated by decreasing the *standby* power consumption, i.e. using more efficient sensors or adaptive sampling. The latter one using a low sampling rate, which can be used to ramp up the sampling process once a signal is detected. However, decreasing the amount of required communication would be more fruitful. An unsolicited data transfer would remove the necessity to keep the RF receiver powered, and still provide real-time feedback when required. Since the data is relatively consistent over large timespan (the flow rate is often fixed for longer periods) a compression scheme could reduce the amount of transmitted data.

CONCLUSIONS

A prototype that is able to capture, process and transmit water usage data of non-digital water meters was developed and presented. Since our system consists of a minimal set of components and does not require an extensive installation, we argue that such a system holds a lot of promise especially for retro-fitting existing (non-digital) water meters.

In a series of evaluations, we tested the sensing and signal processing methods, showing that the measurement accuracy is sufficient for most common water usage tracking applications, where the user can be kept informed about continuous water usage in a real-time fashion.

An infra-red light barrier method, which measures the movement of the cogs of the measuring wheel, was compared to a magnetic method, which picks up the movement of the wet-dry coupling inside water meters. The evaluation shows that the a *zero-crossing* processing of the measured data is sufficient for informing the user about his consumption and that the magnetic approach is more accurate. The infra-red method is limited by missing rotations when opening and closing the valve, which can be fixed by a more complex processing.

Although our proposed system is functioning well as a low-cost and easy to install system for personal feedback on water usage, we also found that our prototype's accuracy is limited and still not high enough to be usable in the calculation of utility bills. However, by providing a more complex processing, this shortcoming can be removed. Furthermore the current system requires too much energy to be useful over longer terms. Future research in this direction will therefore aim at improving the power efficiency of the system by reducing sensor power requirements, as well descreasing communication requirements.

REFERENCES

1. A. L. Sonderlund, J. R. Smith, C. Hutton, and Z. Kapelan, "Using smart meters for households water consumption feedback: Knows and unknowns," *16th Conference on Water Distribution System Analysis*, 2014.
2. J. Froehlich, L. Findlater, and J. Landay, "The design of eco-feedback technology," in *Proceedings of the SIGCHI Conference on Human Factors in Computing Systems*. ACM, 2010, pp. 1999–2008.
3. F. Hofmann, "Principles of electromagnetic flow measurement," 2011. [Online]. Available: http://cdn.krohne.com/dlc/BR_EMF_en_2011.pdf
4. ——, "Fundamentals of ultrasonic flow measurements," 2001. [Online]. Available: http://cdn.krohne.com/dlc/BR_ULTRASONIC_en_72.pdf
5. M. Kompf, "OpenCV Praxis: OCR für den Stromzähler," 2015, [Online; accessed 18-June-2016].

[Online]. Available: https://www.kompf.de/cplus/emeocv.html

6. V. Tasic, T. Staake, T. Stiefmeier, V. Tiefenbeck, E. Fleisch, and G. Tröster, "Self-powered water meter for direct feedback," *Proc. 2012 Int. Conf. Internet Things, IOT 2012*, pp. 24–30, 2012.
7. A. Pericli and J. O. Jenkins, "Smart meters and domestic water usage," University of Hertfordshire, Department of Biological and Environmental Sciences, Tech. Rep., 2015.
8. J. Harou, P. Garrone, A. E. Rizzoli, A. Maziotis, A. Castelletti, P. Fraternali, J. Novak, R. Wissmann-Alves, and P. Ceschi, "Smart metering, water pricing and social media to stimulate residential water efficiency: Opportunities for the smarth2o project," 2014.
9. "Driblet device," 2015, [Online; accessed 19-June-2016]. [Online]. Available: http://www.driblet.io
10. "Fluid water meter," 2015, [Online; accessed 19-June-2016]. [Online]. Available: http://www.fluidwatermeter.com
11. "Intellih20 device," 2015, [Online; accessed 19-June-2016]. [Online]. Available: http://www.intelli-h2o.com/products/technology
12. S. Cheshire and M. Krochmal, "Multicast DNS," RFC 6762 (Proposed Standard), Internet Engineering Task Force, Feb. 2013. [Online]. Available: http://www.ietf.org/rfc/rfc6762.txt
13. I. Fette and A. Melnikov, "The WebSocket Protocol," RFC 6455 (Proposed Standard), Internet Engineering Task Force, Dec. 2011. [Online]. Available: http://www.ietf.org/rfc/rfc6455.txt
14. R. W. Wall, "Simple methods for detecting zero crossing," 2012.
15. S. W. Smith, *The Scientist and Engineer's Guide to Digital Signal Processing*. San Diego, CA, USA: California Technical Publishing, 1997.
16. G. Goertzel, "An algorithm for the evaluation of finite trigonometric series," *The American Mathematical Monthly*, vol. 65, no. 1, pp. 34–35, 1958.
17. A. V. Oppenheim and R. W. Schafer, *Discrete-Time Signal Processing*. Pearson Education, 1999.